

## CHAPTER 3

**Effect of constitutive heterologous overexpression of phosphoenolpyruvate carboxylase (*ppc*) gene of *Synechococcus elongatus* PCC 6301 on physiology and glucose metabolism of *P. fluorescens* ATCC 13525**

*There is only one thing more painful than learning from experience, and that is not learning from experience.*

*-Laurence J. Peter*

### 3.1: INTRODUCTION

Pseudomonads are highly diverse, metabolically and physiologically, as compared to the model organism *E. coli* as discussed in Chapter 1. One of the highly explored junctions in the *E. coli* carbon metabolism is the phosphoenolpyruvate (PEP)-Pyruvate-Oxaloacetate (OAA) node which is the critical branch point between catabolism and anabolism. The carbon flux distribution is regulated by dynamic equilibrium between the metabolites at this junction by the activities of the enzymes which are controlled at both transcriptional and allosteric levels. As compared to *E. coli*, the set of enzymes at the node differ in other organisms like *Bacillus*, *Corynebacterium* and *Pseudomonas citronellolis*. Thus, the flux to and from anaplerotic node in these organisms is differentially regulated which is evident from the nature of metabolic responses to a specific genetic manipulation. For example, in *E. coli* phosphoenolpyruvate kinase (PEPCK) mutant, the anaplerotic flux through phosphoenolpyruvate carboxylase (PPC) was reduced while the glyoxylate shunt was activated where as in *C. glutamicum* it drastically increased the production of lysine and glutamate (Yang et al., 2003; Sauer and Eikmanns, 2005). Overexpression of pyruvate carboxylase (*pyc*) gene in wild type *E. coli* reduced acetate overflow and improved recombinant protein production while in *ppc* mutant *E. coli* and alcohol dehydrogenase (*adhE*)-lactate dehydrogenase (*ldhA*) double mutant *E. coli* resulted in increased succinic acid production (Gokarn et al., 2000; March et al., 2002; Sanchez et al., 2005a). On the contrary, *pyc* overexpression in *C. glutamicum* resulted in growth enhancement or lysine overproduction depending on aspartate kinase activity (Koffas et al., 2002). Similarly, genetic engineering in the form of overexpression of *ppc* gene involved in OAA biosynthesis has been a frequent target for altering the flux at PEP-Pyruvate-OAA node.

#### 3.1.1: Effects of *ppc* gene overexpression in *E. coli* and other organisms

Alteration of the metabolic rigidity and carbon flow at the PEP branch-point by various genetic manipulations including *ppc* overexpression has been well-studied in *E. coli*. Under anaerobic conditions, *ppc* overexpression in *E. coli* altered carbon flux towards fermentation products leading to a significant increase in the yield of succinic acid on glucose which otherwise is a minor product (Millard et al., 1996). Fermentation patterns of *E. coli* overexpressing *ppc* or *pyc* genes suggested that the cell adapted to these genetic alterations by adjusting the flux to lactate, ethanol and acetate (Gokarn et

al., 2000). Under aerobic condition overexpression of *ppc* decreased the rates of glucose consumption and organic acid excretion, but the growth and respiration rates remained unchanged; thereby resulting into improved growth yield on glucose (Chao and Liao, 1993). This result indicated that the wild-type level of PPC was not optimal for the most efficient glucose utilization in batch cultures. Under aerobic conditions in presence of excess glucose, *ppc* overexpression in *E. coli* did not affect the growth and the glucose consumption rates but reduced the acetate excretion by 60% (Farmer and Liao, 1997; Abdel-Hamid et al., 2001). Simultaneous overexpression of *ppk* and *pck*, or *pps* alone in the presence of glucose lead to futile cycling, which did not affect the growth rate significantly (Liao et al., 1994).

*E. coli ppc* gene when expressed in *Synechococcus* PCC 7942 *ppc* mutant showed lower PPC activity with reduced growth, chlorophyll-a content and photosynthetic activity (Luinenburg and Coleman, 1993). Overexpression of *ppc* gene in combination with ornithine carbamoyltransferase and carbamoylphosphate synthetase genes triggered the biosynthesis of cyanophycin in *Acinetobacter sp.* strain ADP1 (Elbahloul and Steinbüchel, 2006). Overexpression of *ppc* gene resulted in lysine overproduction in *C. glutamicum* containing feedback-resistant aspartate kinase while it did not contribute much in glutamate overproduction (Cremer et al., 1991; Shirai et al., 2007).

### 3.1.2: Heterologous *ppc* overexpression in pseudomonads

#### 3.1.2.1: Why *ppc* overexpression in pseudomonads?

Distinct metabolic features in pseudomonads as compared to *E. coli*, in particular the glucose catabolism, suggests different responses to genetic manipulations at the anaplerotic node: (i) Unlike *E. coli*, glucose catabolism in pseudomonads occurs through two alternating pathways, periplasmic direct oxidative and intracellular phosphorylative pathway, both ultimately leading to ED pathway; (ii) PEP is not involved in glucose transport; (iii) OAA can be produced by both PPC and PYC enzymes, the latter being absent in *E. coli* (Gokarn et al., 2000). However as revealed by the genome sequences and other experimental evidences, the occurrence of PPC and PYC is highly variable through different *Pseudomonas* spp. (Table 3.1); (iv) The TCA cycle functions via unusual pyruvate shunt involving ME (Fuhrer et al., 2005); and (v) The acetate overflow metabolism in pseudomonads is negligible as compared to its predominance in *E. coli*.

<i>Pseudomonas</i> strains	PPC	PYC	GDH*	GI Number/Reference
<b>Based on genome sequence</b>				
<i>P. aeruginosa</i> PAO1	+	putative	+	110645304
<i>P. fluorescens</i> Pf-5	+	putative	putative	70728250
<i>P. fluorescens</i> PfO-1	+	-	<i>uc</i>	77456228
<i>P. putida</i> KT2440	+	-	+	26986745
<i>P. putida</i> F1	+	-	-	148545259
<i>P. putida</i> GB-1	+	-	-	166857509
<i>P. aeruginosa</i> UCBPP-PA14	+	putative	+	116048575
<i>P. syringae</i> pv. <i>phaseolicola</i> 1448A	+	+(subunit B)	+	71733195
<i>P. stutzeri</i> A1501	+	+(subunit B)	+	146280397
<i>P. mendocina</i> ymp	+	+(subunit B)	+	46305042
<i>P. entomophila</i> L48	+	+(subunit B)	+	95101722
<i>P. syringae</i> pv. <i>tomato</i> str. DC3000	+	+(subunit B)	putative	28867243
<b>Based on experimental information</b>				
<i>P. fluorescens</i>	+	+	<i>na</i>	Higa et al., 1976
<i>P. citronellolis</i>	+	+	-	O'Brien et al., 1977
<i>P. aeruginosa</i> 640x	+	+	<i>na</i>	Mal'tseva et al., 1982
<i>P. fluorescens</i> 52-1C	-	+	+	Fuhrer et al., 2005
<i>Pseudomonas</i> MA	+	<i>na</i>	<i>na</i>	Newaz and Hersh, 1975

**Table 3.1: Occurrence and distribution of PPC, PYC and GDH enzymes in different *Pseudomonas* species.** \* indicates PQQ dependent GDH; *uc*-existence of the gene is unclear; *na*-information not available. + and - indicate presence or absence of the gene/experimental evidence for all the 3 enzymes. GDH has been included in this comparison as it constitutes a chief glucose catabolic route, the presence or absence of which might correlate with the physiological significance of enzymatic variations at the anaplerotic node.

The enzymes responsible for optimal metabolite balance at the anaplerotic node have been characterized for *Pseudomonas citronellolis* however, it is unexplored with respect to metabolic alterations (O'Brien *et al.*, 1977). On account of significant differences in metabolic framework of *E. coli* and *Pseudomonas* spp. and high

agricultural and environmental importance of pseudomonads, it is necessary to understand the importance of the dynamic anaplerotic node in the central carbon metabolism by performing genetic manipulations at this node.

### 3.1.2.2: Why heterologous *ppc* gene?

PPC, being one of the key enzymes at the critical anaplerotic as discussed earlier, is highly regulated under physiological conditions. Majority of the PPC enzymes of non-photosynthetic bacteria including *E. coli* and *P. citronellolis* belong to class I which get allosterically activated by acetyl-CoA and inhibited by L-aspartate (Newaz and Hersh, 1975; O'Brien *et al.*, 1977). In *E. coli*, additionally PPC is activated by fructose 1, 6-bisphosphate, GTP and long chain fatty acids while is inhibited by L-malate (Morikawa *et al.*, 1980). On the contrary as rare case, PPC in *Pseudomonas* AM-1 and *Pseudomonas* MA grown on methylamine as sole carbon source belonged to Class III as they were independent of acetyl-CoA and aspartate mediated allosteric regulations (Large *et al.*, 1962; Newaz and Hersh, 1975). PPC in *Pseudomonas* MA was also activated by NADH and inhibited by ADP (Millay *et al.*, 1978).

In order to avoid such allosteric regulations exerted at the anaplerotic node by the host metabolism, *ppc* gene from a heterologous host *Synechococcus elongatus* PCC 6301 (*Anacystis nidulans*, cyanobacteria) was selected for the present study. This PPC is known to be non-allosteric and has been demonstrated to be insensitive to the allosteric effectors including dioxane (non-physiological activator) and L-aspartate (Ishijima *et al.*, 1985; Kodaki *et al.*, 1985). Cyanobacterial PPC is not activated by acetyl-CoA (Luinenburg and Coleman, 1993). *S. elongatus ppc* gene codes for a 1053 amino acid residue polypeptide with the codon usage not so markedly different from that of the *E. coli ppc* (Katagiri *et al.*, 1985). Like most of the known PPCs, this cyanobacterial PPC functions as a homotetramer of ~95–110-kDa subunits, and is more closely related to bacterial PPCs due to presence of conserved bacterial type (including *E. coli*) catalytic domain and lack of N-terminal phosphorylation domain typical of plant PPC (Kai *et al.*, 1999; Sanchez and Cejudo, 2003; Xu *et al.*, 2006; Sugita *et al.*, 2007).

This chapter dealt with developing *P. fluorescens* 13525 strain expressing *Synechococcus elongatus* PCC 6301 *ppc* gene and monitoring its effects on the glucose metabolism.

### 3.2: EXPERIMENTAL DESIGN

The experimental plan of work includes the following-

#### 3.2.1: Bacterial strains used in this study

Bacterial strains	Characteristics	Source/Reference
<b><i>E. coli</i> strains</b>		
<i>E. coli</i> JM101	Used for molecular biology experiments	Sambrook and Russell, 2001
<i>E. coli</i> JWK3928	<i>ppc</i> <sup>-</sup> strain used for functional analysis of pAB3 plasmid <i>ppc</i> containing; Km <sup>r</sup>	Peng et al, 2004
JM101 (pAB2)	<i>E. coli</i> JM101 with pAB2 plasmid; Amp <sup>r</sup> , Tc <sup>r</sup>	This study
JM101 (pAB3)	<i>E. coli</i> JM101 with pAB3 plasmid; Amp <sup>r</sup> , Tc <sup>r</sup>	This study
JM101 (pAB4)	<i>E. coli</i> JM101 with pAB4 plasmid; Amp <sup>r</sup> , Tc <sup>r</sup>	This study
JWK3928 (pAB2)	<i>E. coli</i> JWK3928 with pAB2 plasmid; Km <sup>r</sup> , Tc <sup>r</sup>	This study
JWK3928 (pAB3)	<i>E. coli</i> JWK3928 with pAB3 plasmid; Km <sup>r</sup> , Tc <sup>r</sup>	This study
JWK3928 (pAB4)	<i>E. coli</i> JWK3928 with pAB4 plasmid; Km <sup>r</sup> , Tc <sup>r</sup>	This study
<i>Enterobacter asburiae</i> PSI3	Pigeon pea rhizosphere isolate	Gyaneshwar et al., 1999
<b><i>Pseudomonas</i> strains</b>		
<i>P. fluorescens</i> ATCC 13525	Wild type	MTCC, Chandigarh
<i>P. putida</i> KT2440	<i>hsdRI hsdM</i> <sup>+</sup> , Plasmid free derivative of <i>P. putida</i> mt-2	Franklin et al., 1981 Yuste et al., 2006
<i>P. putida</i> BBC443	<i>P. putida</i> SM1443 containing TOL <i>gfp</i> mut3b plasmid expressing GFP; Km <sup>r</sup>	Christensen et al., 1998
<i>P. fluorescens</i> -TOL	<i>P. fluorescens</i> ATCC 13525 containing TOL <i>gfp</i> mut3b plasmid; Km <sup>r</sup>	This study
<i>Pf</i> (pAB3)	<i>P. fluorescens</i> 13525 with pAB3 plasmid; Tc <sup>r</sup>	This study
<i>Pf</i> (pAB4)	<i>P. fluorescens</i> 13525 with pAB4 plasmid; Tc <sup>r</sup>	This study

**Table 3.2: List of bacterial strains used.** Detailed characteristics of these strains are given in Table 2.1; 2.2. Parent strains and the transformants of *E. coli* and *Pseudomonas* were respectively grown at 37°C and 30°C with variations in tetracycline and kanamycin concentrations for rich and minimal media as described in Section 2.2.

### 3.2.2: Expression of *lac* promoter in pseudomonads

*P. putida* BBC443 contained a modified TOL plasmid (~117Kb) conferring several properties to the host, like toluene degradation, kanamycin resistance and green fluorescence due to green fluorescence protein (GFP) cloned under *lac* promoter (Table 3.2; Christensen et al., 1998). Green fluorescence due to GFP expression was monitored in *P. putida* BBC443 and *P. putida* KT2440 on Luria Agar as well as BH Agar containing Na-benzoate as sole carbon source (Section 2.5). Similarly, *P. fluorescens* 13525 which could not utilize aromatic hydrocarbons as carbon source was conjugally transformed with TOL plasmid (Section 2.4.3). The transformants were selected on kanamycin and the positive *P. fluorescens*-TOL plasmid transformants were checked for kanamycin resistant growth and presence GFP mediated fluorescence on BH agar containing Na-benzoate. IPTG was not used to induce *lac* promoter in any of the above experiments.

### 3.2.3: Incorporation of *S. elongatus* PCC 6301 *ppc* gene under *lac* promoter of a pseudomonad stable vector

The pUC based plasmid vector pUCPM18 was used to clone the *ppc* gene of *S. elongatus* PCC 6301 because of its small size, contains multiple cloning sites and has a region that provides mobility and stability in various rhizobacteria (Section 2.1). Since many pseudomonads have ampicillin resistance, it was necessary to incorporate another antibiotic marker gene in addition to *ppc* gene. Hence, the following cloning strategy was employed to incorporate *ppc* gene under *lac* promoter:

#### Step 1: Incorporation of tetracycline resistance gene downstream to *ppc* gene of *S. elongatus* PCC 6301

The tetracycline resistance gene (*tc'*) was incorporated downstream to the *ppc* gene in pA172A plasmid (Table 2.3) as a selection marker. The *tc'* gene fragment, containing *tetA-tetR* genes, was obtained from pME6010 plasmid by digesting with BamHI and BglII (Section 2.1). The 2,817bp fragment containing *tc'* was ligated to the purified BamHI digested pA172A plasmid to obtain the recombinant pAB1 plasmid of 10,716bp. The ligation mixture was transformed into *E. coli* JM101 strain and the transformants were selected on agar plates containing ampicillin and tetracycline. The plasmid isolated from the transformants was confirmed for the presence of *tc'* by restriction digestion with BamHI, KpnI, EcoRV and HindIII enzymes. Being a single site

cloning event, the orientation of the *tc<sup>r</sup>* in pAB1 was selected such that it allowed the excision of both *ppc* gene as well as *tc<sup>r</sup>* gene in a HindIII fragment.

### **Step 2: Incorporation of the HindIII fragment containing both *ppc* gene of *S. elongatus* PCC 6301 and *tc<sup>r</sup>* in pseudomonas stable vector, pUCPM18**

The pAB1 plasmid was digested with HindIII to obtain the 6,658bp fragment having *S. elongatus* PCC 6301 *ppc* gene followed by tetracycline resistance gene, *tc<sup>r</sup>*. This 6,658bp HindIII fragment was gel eluted and ligated to purified pUCPM18 plasmid digested with HindIII, to obtain the resultant 12,007bp plasmid. The ligation mixture was transformed in *E. coli* JM101 and the transformants were selected on agar plates containing ampicillin and tetracycline. Since it was non-directional cloning, the 6,658bp insert could get ligated in two different orientations. In one orientation *ppc* gene would contain only *tet* promoter (pAB2) while in the other orientation the *lac* promoter would be closely located at the upstream of *tet* promoter (pAB3). The orientation of the insert in both pAB2 and pAB3 plasmids was confirmed by the restriction digestion patterns with XbaI, KpnI, HindIII and BamHI.

The BamHI-BglII fragment of 2,817bp containing *tc<sup>r</sup>* was ligated to BamHI linearized pUCPM18 plasmid to obtain 8,166bp control plasmid. The ligation mixture was transformed in *E. coli* JM101 strain and the transformants were selected on ampicillin and tetracycline plates. Opposite orientation of the insert in the resultant pAB4 and pAB5 plasmids was confirmed by restriction digestion with PstI, HindIII and KpnI enzymes.

All the molecular biology techniques like plasmid DNA isolation and transformation, restriction digestion, gel elution and purification, DAN ligation and gel electrophoresis were performed as described in Section 2.4.

#### **3.2.4: Functional confirmation of PPC expressed from pAB2 and pAB3**

*E. coli* strain JWK3928, which exhibited glutamate auxotrophy due to mutation in *ppc* gene, was used for determining the functionality of the *ppc* gene in pAB2 and pAB3. The control plasmid pAB4 along with pAB2 and pAB3 were transformed into *E. coli* JWK3928 (Table 3.2; Section 2.4.2.1). The transformants on agar plates containing kanamycin and tetracycline confirmed the presence of respective plasmids and then these

strains were subjected to auxotrophy complementation studies (Section 2.8). *E. coli* JM101 harboring pAB2, pAB3 and pAB4 plasmids were subjected to SDS-PAGE analysis (Section 2.4.8) to confirm the presence of heterologous PPC protein.

### **3.2.5: Development of *P. fluorescens* 13525 harboring *ppc* gene of *S. elongatus* PCC 6301**

The recombinant plasmids pAB3 and pAB4 (control) were transformed in *P. fluorescens* 13525 (Section 2.4.2.2). The transformants were selected on tetracycline selection plates and were confirmed by fluorescence and citrate utilization (Section 2.6).

### **3.2.6: Effect of heterologous *ppc* gene expression on the physiology and glucose metabolism**

*P. fluorescens* transformants were subjected to physiological experiments involving growth and organic acid production profiles on M9 minimal medium with 0.2%, 30mM and 100mM glucose as carbon source (Section 2.9; 2.2.3). The samples withdrawn at regular interval were analyzed for O.D.<sub>600nm</sub>, pH, extracellular glucose and organic acid (Section 2.9.3). The physiological parameters were calculated as in Section 2.9.3. The enzyme assays were performed as described in Section 2.10; with PPC, PYC, G-6-PDH and GDH being assayed in mid-log to late-log phase cultures while CS, ICL and ICDH being assayed in the stationary phase cells.

## **3.3: RESULTS**

### **3.3.1: Use of *lac* promoter for constitutive expression of desired genes in pseudomonads**

Lactose utilization of the *P. fluorescens* 13525, *P. putida* KT2440 and *P. putida* BBC443 strains was checked on M9 minimal medium supplemented with lactose as sole carbon source (Section 2.6). None of the *Pseudomonas* strains and *E. coli* JM101 (used as negative control) could grow on lactose whereas *Enterobacter asburiae* PSI3 showed good growth (utilizes lactose; used as a positive control) as shown in Fig 3.1.

*P. putida* BBC443 containing TOL*gfp*mut3b plasmid could grow and fluoresce due to GFP expression from *lac* promoter on rich media like Luria Agar as well as BH

agar with Na-benzoate as sole carbon source in the presence of kanamycin. On the contrary, *P. putida* KT2440 lacking pTOL plasmid grew on Luria Agar but could not fluoresce while failed to utilize Na-benzoate in the presence of kanamycin (Fig. 3.2). On the other hand, conjugal transfer of pTOL from *P. putida* BBC443 to *P. fluorescens* 13525 not only imparted the ability to utilize Na-benzoate as the sole carbon source in presence of kanamycin and but also conferred GFP expression as evident from green fluorescence (Fig. 3.2). These results confirmed that *lac* promoter was constitutively functional and thus could be used to express foreign genes in *Pseudomonas* strains.

**Fig. 3.1: Lactose utilization of *Pseudomonas* strains on M9 minimal medium.** 1: *P. fluorescens* ATCC 13525; 2: *P. putida* BBC443 (+TOL*gfp*mut3b plasmid); 3: *P. putida* KT2440; 4: *E. coli* JM101, 5: *Enterobacter asburiae* PS13

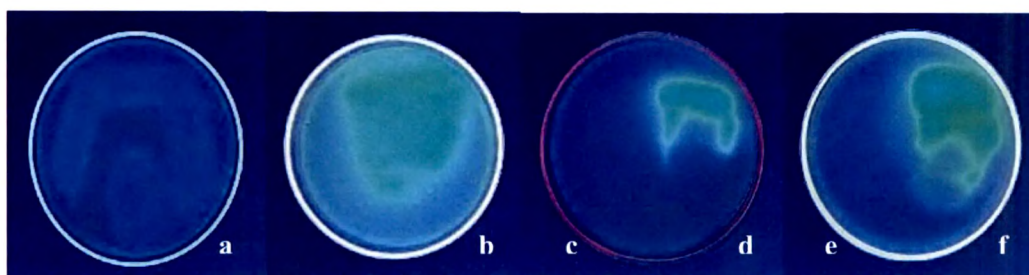


**Fig. 3.2: pTOL mediated Na-benzoate utilization and GFP expression in *Pseudomonas* strains.** Growth and GFP mediated fluorescence of (a) *P. putida* KT2440 on Luria Agar, (b) *P. putida* BBC443 (+TOL*gfp*mut3b plasmid) on Luria agar, (c), (d), (e) and (f) *P. putida* KT2440, *P. putida* BBC443 (+TOL*gfp*mut3b plasmid), *P. fluorescens* 13525 and *P. fluorescens*-TOL (+TOL*gfp*mut3b plasmid) respectively on BH Agar containing Na-benzoate as sole carbon source and 7.5µg/ml kanamycin.

### 3.3.2: Construction of *Pseudomonas* stable plasmid containing *ppc* gene of *S. elongatus* PCC 6301 under *lac* promoter

Based on the strategy discussed above (Section 3.2.3), pAB3 plasmid containing both *ppc* and *tc<sup>r</sup>* genes incorporated in pUCPM18 was selected to have *ppc-tc<sup>r</sup>* fragment

under *lac* promoter. The insertion of *ppc-tc'* fragment in other orientation was expected to be under *tet* promoter of pBR322 (pAB2). The schematic representation of the cloning procedures discussed in section 3.2.3 is depicted in Fig. 3.3. The control vector was also developed through single-site cloning and plasmids containing *tc'* in both orientations, pAB4 and pAB5, were obtained of which pAB4 was used henceforth as the vector control for all further experiments. All the plasmids were confirmed based on restriction digestion pattern (Fig. 3.4a, b, c and d) and were subjected to various confirmatory experiments to indicate expression of functional *ppc* gene before using for developing the *Pseudomonas* transformants.

### 3.3.3: *E. coli ppc* mutant complementation studies

*E. coli ppc* mutant strain harboring the pAB2, pAB3 and pAB4 plasmids were subjected to growth on M9 minimal medium containing glucose as carbon source. *E. coli ppc* mutant strain harboring pAB3 could grow on glucose without glutamate supplementation unlike the control pAB4 (Fig. 3.5). However, pAB2 could not complement the *ppc* mutant phenotype.

### 3.3.4: SDS-PAGE analysis of the *E. coli* JM101 transformants carrying pAB2, pAB3 and pAB4 recombinant plasmids

The PPC protein of *S. elongatus* PCC 6301 is known to function as a homotetramer. Size of cyanobacterial PPC monomer is ~110kDa while that of the *E. coli* is known to be ~95kDa (Millard et al., 1996; Kodaki et al, 1985). Cell free extracts of *E. coli* JM101 transformants of pAB2, pAB3 and pAB4 were analyzed through SDS-PAGE (Fig. 3.6). *E. coli* JM101 containing pAB3 induced with 1mM IPTG showed an intense band at ~110kDa position. But no band corresponding to PPC was observed in case of pAB4 control and pAB2 transformants.

Inability of pAB2 to complement the *ppc* mutant phenotype and absence of the band at expected size indicated non-functional status of pAB2. Further investigations on pAB2 revealed that a HindIII site used to obtain *ppc-tc'* fragment, disrupted the *tet* promoter thereby failing to express *ppc* gene. Therefore, the transformants of *P. fluorescens* 13525 were developed using pAB3 only which had *ppc* gene under *lac* promoter and pAB4 (negative control) and were subjected to detailed physiological studies.



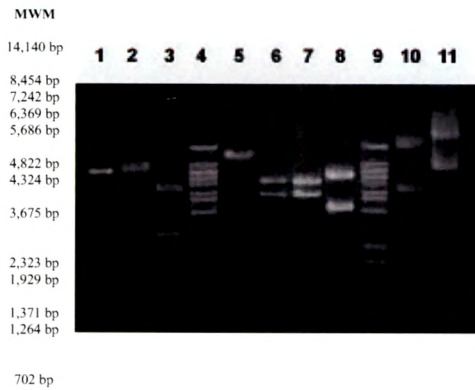


**Fig. 3.4a: Restriction digestion pattern for pAB1.**

Lane 1: pA172A digested with BamHI (7,968bp); Lane 2: pME6010 digested with BamHI (8,270bp); Lane 3: pME6010 digested with BamHI-BglII (5,453bp, 2,817bp); Lane 4: Molecular Weight Marker (MWM)-Lambda DNA cut with BstEII; Lane 5: pAB1 linearised with BamHI (10,716 bp); Lane 6: pAB1 digested with KpnI (6,098 bp, 4,618 bp); Lane 7: pAB1 digested with EcoRV (6,125bp, 4,591bp); Lane 8: pAB1 digested with HindIII (6,658bp, 4,058bp); Lane 9: MWM-Lambda DNA cut with BstEII; Lane 10: pA172A plasmid undigested; Lane 11: pAB1 plasmid undigested

**Fig. 3.4b: Restriction digestion pattern for pAB2.**

Lane 1: pUCPM18 digested with HindIII (5,349bp); Lane 2: pAB1 linearized with BamHI (10,716bp); Lane 3: pAB1 digested with HindIII (6,658bp, 4,058bp); Lane 4: MWM-Lambda DNA cut with BstEII; Lane 5: pAB2 linearised with XbaI (12,007bp); Lane 6: pAB2 digested with BamHI (9,203bp, 2,804bp); Lane 7: pAB2 digested with KpnI (7,372bp, 4,635bp); Lane 8: pAB2 digested with HindIII (6,658bp, 5,349bp); Lane 9: MWM-Lambda DNA cut with BstEII; Lane 10: pUCPM18 plasmid undigested; Lane 11: pAB2 plasmid undigested



**Fig. 3.4c: Restriction digestion pattern for pAB3.**

Lane 1: pUCPM18 digested with HindIII (5,349bp); Lane 2: pAB1 linearized with BamHI (10,716bp); Lane 3: pAB1 digested with HindIII (6,658bp, 4,058bp); Lane 4: MWM-Lambda DNA digested with BstEII; Lane 5: pAB3 linearised with XbaI (12,007bp); Lane 6: pAB3 digested with BamHI (8,093bp, 3,914bp); Lane 7: pAB3 digested with KpnI (9,906bp, 2,101bp); Lane 8: pAB3 digested with HindIII (6,658bp, 5,349bp); Lane 9: MWM-Lambda DNA cut with BstEII; Lane 10, 11: pUCPM18 plasmid undigested; Lane 11: pAB3 plasmid undigested.

**Fig. 3.4d: Restriction digestion pattern for pAB4 and pAB5.**

Lane1: pUCPM18 digested with HindIII (5,349bp); Lane2: pME6010 linearized with KpnI (8,270bp); Lane3: pME6010 digested with BamHI-BglII (5,453bp, 2,817bp); Lane4: MWM-Lambda DNA digested with BstEII; Lane5: pAB4 linearised with PstI (8,166bp); Lane6: pAB4 digested with KpnI (5,361bp, 2,805bp); Lane7: pAB4 digested with HindIII (8,093bp, 73bp); Lane8: pAB5 linearized with PstI (8,166bp); Lane9: pAB5 digested with KpnI (8,135bp, 31bp); Lane10: pAB5 digested with HindIII (5,352bp, 2,904bp) Lane11,12,13: pAB4, pUCPM18 and pAB5 undigested plasmids



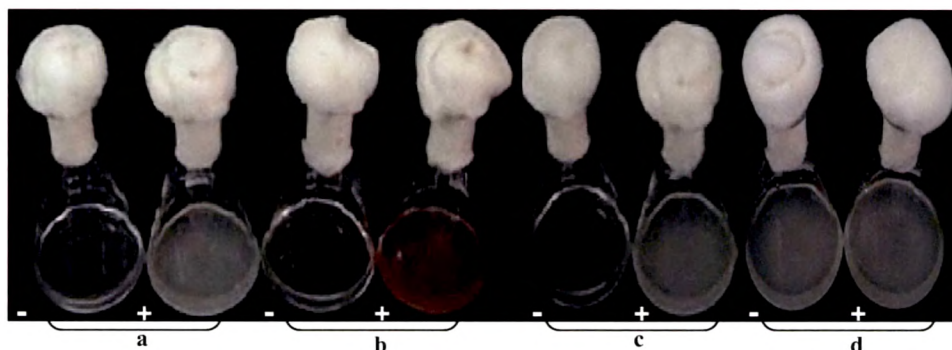


**Fig. 3.5: Complementation of *E. coli* JWK3928 mutant phenotype by pAB3 and pAB4 plasmids.** a: *E. coli* JWK3928-deletion mutant of *ppc* gene b: *E. coli* JWK3928 with pAB4 plasmid c: *E. coli* JWK3928 with pAB2 plasmid; d: *E. coli* JWK3928 with pAB3 plasmid induced with 0.1mM IPTG. Growth is monitored on M9 medium with 0.2% glucose (Section 2.8.). -/+ at the left-bottom corners of each image indicates absence and presence of 340µg/ml glutamate respectively. Other experimental details are as described in Section 2.8. The parent plasmids pA172A and the intermediate construct pAB1 could also complement the *ppc* mutant phenotype (data not shown)

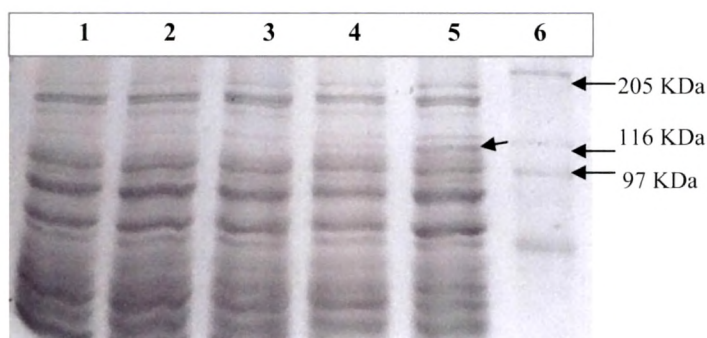


**Fig. 3.6: SDS-PAGE analysis of the *E. coli* JM101 transformants containing the recombinant plasmids.** Lane 1: *E. coli* JM101 containing pAB4 (control); Lane 2: *E. coli* JM101 containing pA172A (Table 3.2); Lane 3: *E. coli* JM101 containing pAB2; Lane 4: *E. coli* JM101 containing pAB3- uninduced; Lane 5: *E. coli* JM101 containing pAB3- induced with 1mM IPTG; Lane 6: Sigma protein molecular weight marker SDS6H2-(30,000-200,000). All the cultures were grown in 3ml LB with respective antibiotics with overnight shaking and were processed for sample preparation. Equal amount of protein was loaded in all the wells for appropriate comparison. Other experimental details are as given in Section 2.4.8.

### 3.3.5: Heterologous overexpression of *S. elongatus* PCC 6301 *ppc* gene in *P. fluorescens* 13525

The PPC activity estimated in *P. fluorescens* 13525 harboring pAB3 {*Pf*(pAB3)} grown on M9 minimal medium with 100mM glucose, was  $50.03 \pm 1.95$ U which was ~12 fold higher than that in control *Pf*(pAB4) which possessed very negligible levels of PPC activity ( $4.12 \pm 0.49$ U). The copy numbers of pAB3 and pAB4 in *P. fluorescens* 13525 was found to be approximately 10 and 14 respectively (detailed in Chapter 6).

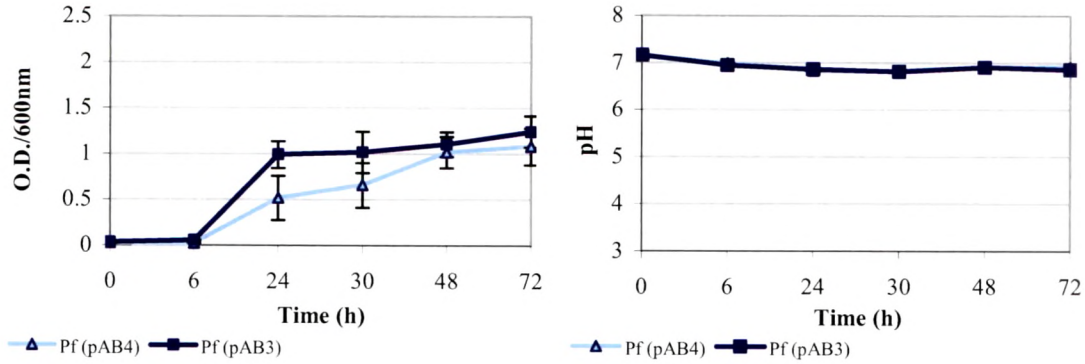
### 3.3.6: Effect of *S. elongatus* PCC 6301 *ppc* overexpression on growth pattern and pH profile in presence of different glucose concentrations

The growth profiles and organic acid secretion of *Pf*(pAB3) and *Pf*(pAB4) on M9 minimal medium demonstrated that at glucose concentration as low as 0.2% (11.11mM), *Pf*(pAB3) had slightly improved growth as compared to its control *Pf*(pAB4) (Fig. 3.7a). With increase in glucose levels *i.e.* at 30mM and 100mM, *Pf*(pAB3) did not display significantly altered growth profile as compared to *Pf*(pAB4) (Fig. 3.7b, c). The maximum cell densities attained increased with increase in glucose concentration. At 0.2% and 30mM glucose, no significant acid production was monitored even after shaking for 72h as suggested from the pH profile (Fig. 3.7a, b). Significant media acidification was monitored only in presence of 100mM glucose that too within 28h. Hence, further detailed analysis of physiological and biochemical parameters was done using M9 minimal medium with 100mM glucose, at which significant organic acid production was found (Fig. 3.7c). However, both *Pf*(pAB3) and *Pf*(pAB4) could not acidify the medium when grown on M9 medium with 100mM fructose (data not shown).

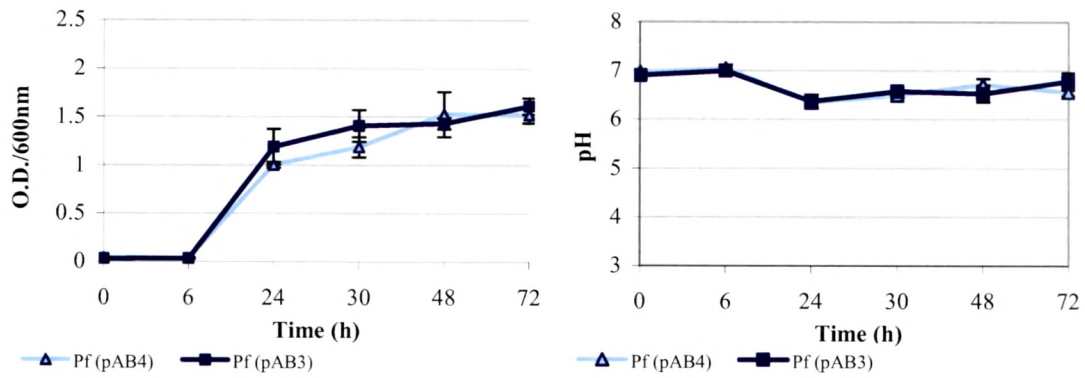
### 3.3.7: Physiological effects of *S. elongatus* PCC 6301 *ppc* overexpression on M9 minimal medium with 100mM glucose

In presence of excess glucose, increase in PPC activity did not significantly affect growth profile (Fig. 3.7c). The specific growth rate, total glucose utilization rate and the total amount of glucose used at the time of pH drop remained unaffected (Table 3.3). However, the amount of glucose consumed intracellularly reduced by about 1.3 fold in *Pf*(pAB3) as compared to *Pf*(pAB4) control. Strikingly the increase in PPC activity improved the biomass yield of *Pf*(pAB3) by ~1.7 fold.

**(a) 0.2% (11.11mM) glucose**



**(b) 30mM glucose**



**(c) 100mM glucose**

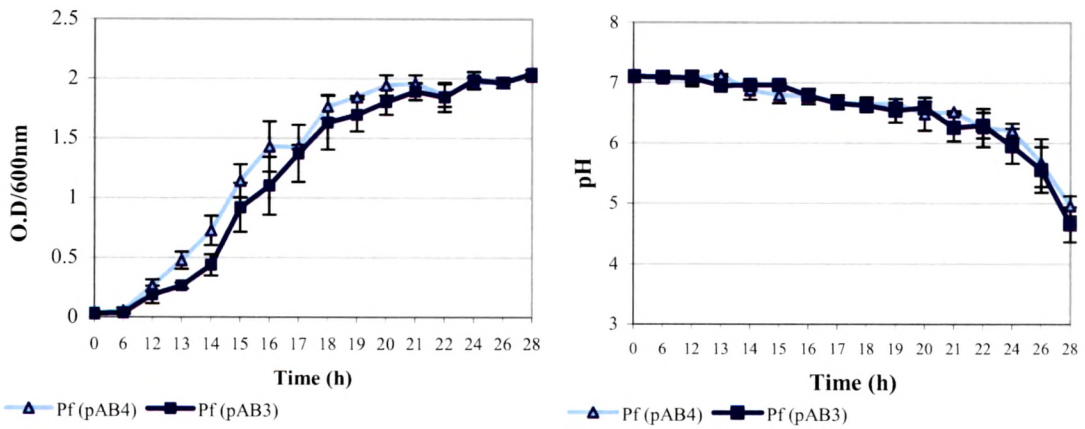


**Fig. 3.7: Growth and pH profiles of *P. fluorescens* 13525 transformants on M9 minimal medium with different glucose concentrations.** The values plotted represent the Mean  $\pm$  S.D of 4-12 independent observations.

Bacterial Strain	Sp. growth rate $k$ ( $h^{-1}$ ) <sup>a</sup>	Total glucose utilized (mM) <sup>b</sup>	Glucose consumed (mM) <sup>b</sup>	Biomass yield $Y_{dcw/Glc}$ (g/g) <sup>a</sup>	Sp. glucose utilization rate $Q_{Glc}$ (g.g dcw <sup>-1</sup> .hr <sup>-1</sup> ) <sup>a</sup>
<i>Pf</i> (pAB4)	0.75 ± 0.04	55.90 ± 2.86	49.61 ± 2.63	0.10 ± 0.01	10.10 ± 1.43
<i>Pf</i> (pAB3)	0.71 ± 0.04 ns	49.17 ± 2.40 ns	<b>39.14 ± 3.33</b> *	<b>0.17 ± 0.02</b> ***	9.96 ± 1.33 ns

**Table 3.3: Physiological variables and metabolic data from *P. fluorescens* 13525 *ppc* transformant grown on M9 medium with 100mM glucose.** The results are expressed as Mean±S.E.M of 6-10 independent observations. <sup>a</sup> Biomass yield  $Y_{dcw/Glc}$ , specific growth rate ( $k$ ) and specific glucose utilization rate ( $Q_{Glc}$ ) were determined from mid log phase of each experiment. <sup>b</sup> Total glucose utilized and glucose consumed were determined at the time of pH drop (28h). The difference between total glucose utilized and glucose consumed is as explained in Section 2.9.3. \* P<0.05, \*\*\* P<0.001, ns=non-significant

### 3.3.8: Biochemical effects of *ppc* overexpression on M9 minimal medium with 100mM glucose

Biochemical effects include the qualitative and quantitative characterization of organic acids secreted as well as the enzymatic parameters.

#### (i) Organic acid secretion

On M9 medium in presence of excess glucose, the organic acids identified were mainly gluconic, pyruvic and acetic acids. As a result of *ppc* overexpression, there was only quantitative change in the organic acids secreted. Extracellular medium of *Pf* (pAB3) contained ~1.6 fold higher amount of gluconic acid, as compared to *Pf* (pAB4) with specific gluconic acid yield,  $Y_{G/G}$ , increasing by 1.5 fold (Fig. 3.8a, b and c). Concomitantly, *Pf* (pAB3) had about 2.3 and 2.5 folds reduction in levels of pyruvic and acetic acids respectively as compared to *Pf* (pAB4) with their corresponding yields ( $Y_{P/G}$  and  $Y_{A/G}$ ) decreasing by 2.2 and 1.9 folds respectively. Extracellular as well as intracellular citric acid levels and yields remained unaltered.

#### (ii) Alterations in enzyme activities in *Pf* (pAB3)

In order to correlate the alterations in physiological variables and organic acid profile, enzymes involved periplasmic direct oxidation and intracellular phosphorylative pathways of glucose catabolism along with PYC, participating in anaplerotic reactions,

were estimated. In response to about 12 fold increase in PPC activity in *Pf* (pAB3), interestingly, GDH activity increased by about 2.5 fold as compared to the control (**Fig. 3.9**). G-6-PDH, estimated to represent the contribution of phosphorylative pathway, and PYC remained unaltered in *Pf* (pAB3) as compared to *Pf* (pAB4). The activities of TCA cycle enzymes, CS and ICDH, in *Pf* (pAB3) did not alter significantly as compared to the control. Glyoxylate pathway enzyme ICL, which may compete with ICDH for the TCA cycle intermediate isocitrate, showed very low activity in both *Pf* (pAB3) and *Pf* (pAB4) and remained unchanged in response to increased PPC activity.

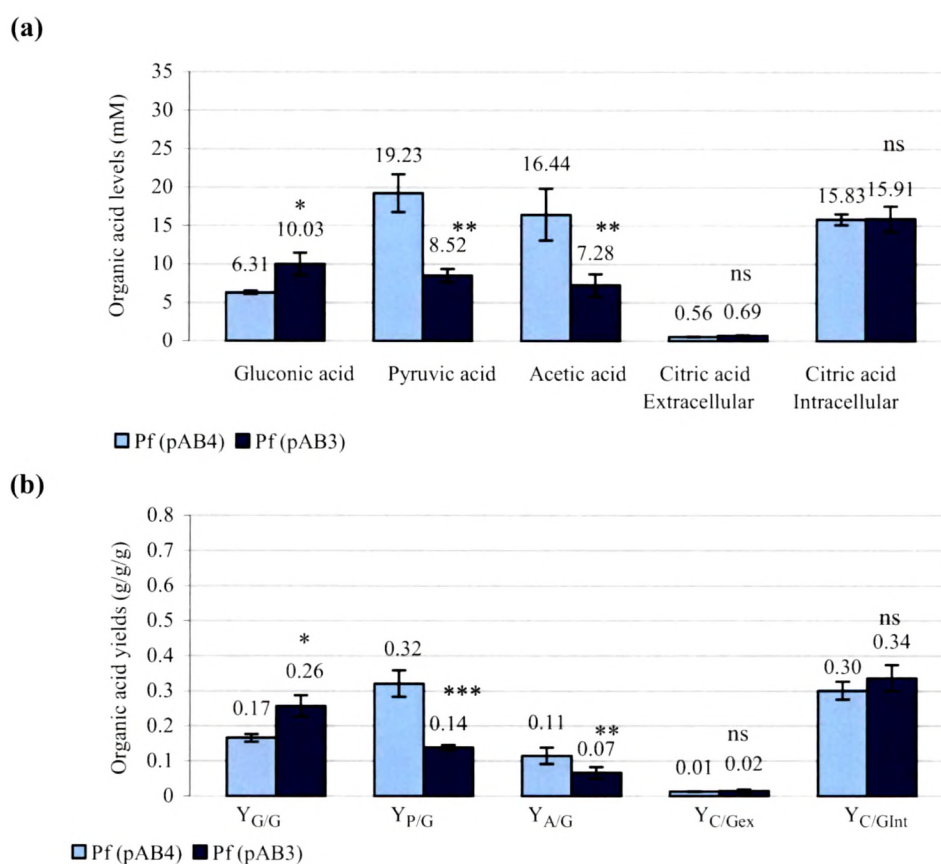


**Fig. 3.8: Organic acid production from *P. fluorescens* 13525 *ppc* transformant.** (a) and (b) depicts the levels and yields of extracellular gluconic, pyruvic, acetic acid, citric acid and intracellular citric acid ( $Y_{G/G}$ ,  $Y_{P/G}$ ,  $Y_{A/G}$ ,  $Y_{C/Gex}$ , and  $Y_{C/GInt}$  respectively) in the late stationary phase cultures of *Pf* (pAB4) and *Pf* (pAB3) grown on M9 minimal medium with 100mM glucose (samples drawn at 28h; Section 2.9; 2.11). Organic acid yields are expressed as g/g of glucose utilized/g dry cell weight. Results are expressed as Mean  $\pm$  S.E.M of 4-8 independent observations. \*  $P < 0.05$ , \*\*  $P < 0.01$ , \*\*\*  $P < 0.001$ , ns=non-significant

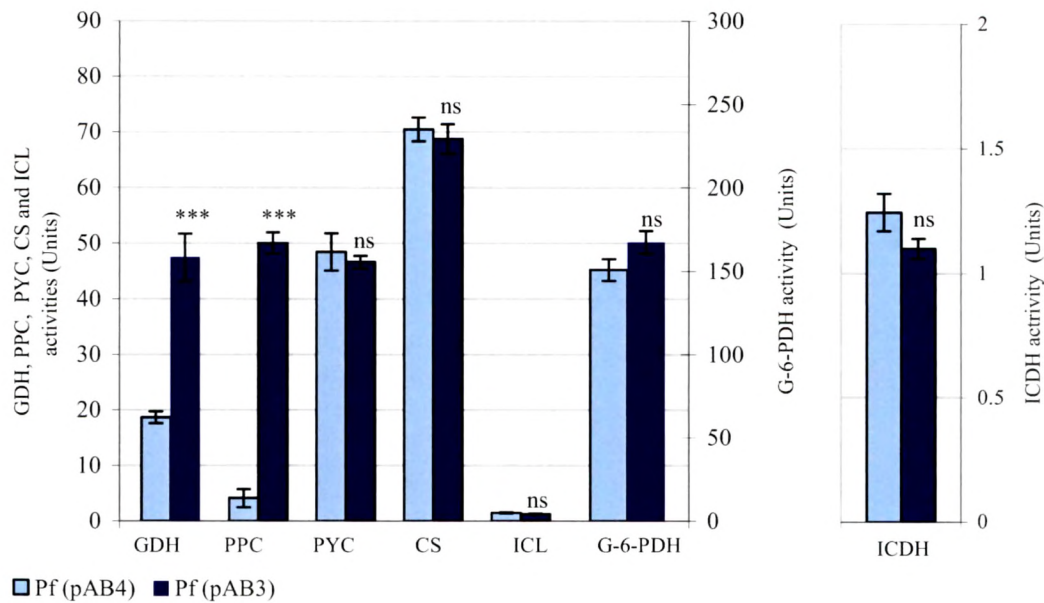


**Fig. 3.9: Activities of enzymes PPC, PYC, GDH, G-6-PDH, ICDH and ICL in *P. fluorescens* 13525 *ppc* transformant.** The activities have been estimated using cultures grown on M9 minimal medium with 100mM glucose. All the enzyme activities were estimated from mid log phase to late log phase cultures except CS, ICDH and ICL which were estimated in stationary phase (Section 2.10). All the enzyme activities are represented in the units of nmol/min/mg total protein, except ICDH activity which is depicted in the units of  $\mu$ mol/min/mg total protein. The values are depicted as Mean $\pm$ S.E.M of 7-10 independent observations. \*\*\* P<0.001, \*\* P<0.01, ns= non-significant.

### 3.4: DISCUSSION

Genetic manipulations altering the carbon flow at the PEP branch-point has been well-studied in *E. coli*, with PPC being a frequent target (Sauer and Eikmanns, 2005). In this study, we report the consequences of *lac* promoter driven *S. elongatus* PCC 6301 *ppc* gene overexpression on glucose catabolism of *P. fluorescens* 13525. Presence of distinct ~110kD band in *E. coli* pAB3 transformant as demonstrated by SDS-PAGE analysis and functional complementation of *E. coli ppc* mutant demonstrated the expression of a functional PPC protein. However, similar studies demonstrated that pAB2 plasmid, which was expected to have *ppc* gene under *tet* promoter, failed to

express *ppc* gene. This could be probably due to disruption of *tet* promoter in the HindIII fragment containing *ppc* and *tc'* genes, derived from pAB1 (pBR322 based) for constructing pAB2 plasmid. This is supported by earlier report demonstrating disruption and inactivation of *tet* promoter of pBR322 plasmid by HindIII digestion (Harley et al., 1988). About 14 fold increase in PPC activity in *P. fluorescens* harboring pAB3 plasmid {*Pf* (pAB3)} was well in accordance with the reports that the *lac* promoter is constitutively active (Table 3.4) and a strong promoter in *Pseudomonas* strains (Table 3.5). The inability of pseudomonads including *P. fluorescens* 13525 to assimilate lactose and absence of glucose mediated cAMP dependent catabolite repression for utilization of any other sugar also justify the constitutive expression of *ppc* gene from *lac* promoter (Lessie and Phibbs, 1984; Basu et al., 2006).

Plasmids	<i>E. coli</i>	<i>P. fluorescens</i> ST	<i>P. putida</i> KT2442
pPR9TT (promoterless)	0.1%	0.02%	0.02%
<b>pPR9TTTrc</b>	<b>100%<sup>a</sup></b>	<b>92%</b>	<b>100%<sup>a</sup></b>

**Table 3.4: Expression of *lacZ* from the *Ptrc* promoter in species other than *E. coli*** (Santos et al., 2001). <sup>a</sup>100% corresponds to 18378±329 Miller units

Plasmid (promoter)	$\beta$ Gal <sup>a</sup> in <i>E. coli</i>	$\beta$ Gal <sup>a</sup> in <i>P. putida</i>
pML122 <i>lac</i> ( <i>pNm</i> )	1400	16300
pML130 <i>lac</i> ( <i>plac</i> )	2000	<b>9800</b>
pML132 <i>lac</i> ( <i>ptac</i> )	<b>11300</b>	2950
pML140 <i>lac</i> ( <i>pSl</i> )	40	3350
without plasmid	16	150

**Table 3.5:  $\beta$ -Galactosidase activities of vectors carrying the *lacZ* gene under different promoters in Gram-negative hosts** (Labes et al., 1990): <sup>a</sup>  $\beta$  Gal activity was determined in the log phase ( $A_{600nm}$ : 0.2-0.6) according to Miller (1972).

Negligible PPC activity detected in control *Pf* (pAB4) necessitated the estimation of yet another OAA biosynthetic enzyme, PYC, whose activity was significantly high. Considering the variations in the occurrence and distribution of *ppc* and *pyc* genes in different *Pseudomonas* sp. and strains studied so far (Table 3.1), *P. fluorescens* 13525 most probably belongs to the group which does not have functional PPC and intracellular OAA is mainly supplied by PYC. Hence, heterologous *ppc* overexpression in *P.*

*fluorescens* would allow the carbon flow into an otherwise negligible pathway with very low flux (Fuhrer et al., 2005) with reduced influence of the allosteric regulations operating for anabolic and catabolic pathways at the PEP/OAA level. Moreover, identification of *Pseudomonas* metabolic network also demonstrated that the glucose flux through TCA cycle in *P. fluorescens* is relatively higher than in *E. coli*. Such a metabolic and genetic background would be expected to allow the enforced increase in PPC activity to affect the flux distribution at the PEP-Pyruvate-OAA junction and the TCA cycle.

In the presence of low glucose levels, although sufficiently high cell densities were attained, there was no acidification which is expected from the low contribution of direct oxidation pathway under these conditions (Quay et al., 1972). However, under low glucose conditions *ppc* overexpression appears to impart growth advantage. In presence of excess glucose, *ppc* overexpression enhanced the biomass yield without affecting the aerobic growth and with ~20% reduction in glucose consumption. Unaltered growth rate could be correlated with unaltered G-6-PDH activity since in *E. coli* increase in growth rate was accompanied by increased G-6-PDH activity (Wolf et al, 1979). Similar results have been reported for *E. coli*, where under aerobic conditions overexpression of *ppc* gene by as low as 7 folds (Farmer and Liao, 1997) to as high as 70 fold (Holms, 2001) had no significant effect on growth even though the specific glucose consumption rate was reduced by about 30%. In contrast to plasmid-borne *ppc* overexpression, 20% reduction in growth rate of *E. coli* was found in response to *ppc* overexpression which was achieved by replacing the natural *ppc* gene promoter with an artificial constitutive promoter (De Mey et al., 2007). In *E. coli*, reduction in glucose consumption was attributed to decreased PEP/pyruvate ratio which in turn could decrease PEP-PTS dependent glucose uptake. Contradictorily, reduction in glucose consumption rate was also reported for *E. coli ppc* mutant (Peng et al., 2004). These observations taken together with our results of *P. fluorescens* overexpressing *ppc* gene (PEP-PTS independent glucose transport), suggest that the effect of altered PPC flux on glucose consumption is independent of the mechanisms underlying glucose transport.

Reduced glucose consumption for intracellular phosphorylative oxidation was counteracted by enhanced direct oxidation pathway as demonstrated by increase in the gluconic acid yield which could be explained by concomitant increase in GDH activity.

This effect on GDH activity could not be compared with *E. coli* as it does not possess a functional direct oxidation pathway (van Schie *et al.*, 1985). Reduced yields of the metabolic by-products like pyruvate and acetate without causing significant alterations in growth rate and marginal decrease in glucose consumption indicated reduced carbon overflow. Similarly, increased GDH activity in *B. subtilis* resulted in reduced acetate and pyruvate production without affecting the glucose consumption (Zhu *et al.*, 2006). Pyruvate secretion is prominently observed for *P. fluorescens* as compared to *E. coli* probably because of major contribution of pyruvate-malate shunt which converts malate to pyruvate and pyruvate to OAA; the reactions subsequently catalyzed by malic enzyme and PYC respectively (Fuhrer *et al.*, 2005). This shunt thus bypasses the regular TCA cycle step of malate conversion to OAA. Pyruvate secretion is unusual to *E. coli*, which secretes pyruvate generally in the conditions where acetate biosynthesis pathways are blocked (Diaz-Ricci *et al.*, 1991; Moreau, 2004).

The absolute enzyme activities of G-6-PDH, PYC and CS which subsequently function for glucose catabolism, at anaplerotic node and TCA cycle generally suggest that once glucose is uptaken maximum flux is through G-6-PDH (150U). Following this, only ~45U of PYC activity contributed at the anaplerotic node which probably was insufficient to completely utilize the pyruvate produced in the upstream ED pathway. Hence although CS activity was relatively higher (~70U), the check at PYC level resulted in pyruvate overflow in *Pf* (pAB4) and incomplete carbon utilization. Enforced increase in OAA biosynthesis by *ppc* overexpression alleviated this check, diverted the PEP towards anabolism and indirectly reduced pyruvate accumulation and overflow. Moreover unlike *E. coli*, the acetate secretion is known to be low in *P. fluorescens* (Fuhrer *et al.*, 2005) and *ppc* overexpression further reduced it. The reduced acetate levels might be due to diversion of the carbon units to meet the increasing demands for metabolites like glucose-6-phosphate, fructose-6-phosphate, ribose-5-phosphate, PEP and pyruvate in biosynthesis as a result of increased biomass (Farmer and Liao, 1997). Collectively, *ppc* overexpression improved metabolic status with respect to more efficient glucose utilization, reduced carbon wastage and diversion of increased OAA pool towards anabolic reactions.

Unaltered CS activity and intracellular as well as extracellular citrate levels suggest that increase in OAA biosynthetic activity in the form of *ppc* overexpression

probably could not divert the increased OAA pool towards TCA cycle, although the basal CS activity and overall TCA cycle flux are known to be higher in pseudomonads than in *E. coli*. These observations taken together with the observed increase in biomass emphasize on anaplerotic role of PPC in *P. fluorescens* in spite of the presence of PYC and that the enzymatic machinery at the anaplerotic node is not fully optimized for efficient glucose utilization (Farmer and Liao, 1997). Similarly, in *E. coli* flux through TCA cycle was unaffected in presence of increased PPC activity (Holms, 2001). Unaltered ICDH activity in *Pf* (pAB3) also indicated that TCA cycle is not significantly affected. However, in *E. coli*, PEP is shown to modulate ICDH and ICL activities *in vitro* however; its *in vivo* significance is unclear (Ogawa et al., 2007). Very low ICL activity suggests negligible contribution of glyoxylate pathway at high glucose levels which is in agreement with repression of ICL activity in presence of glucose in *P. aeruginosa* PAO1 and *P. indigofera* (Howes and McFadden, 1962; Diaz-Perez et al., 2007).

In presence of glucose, the reverse flux from OAA to PEP in *P. fluorescens* is reportedly as high as 17% as compared to 3% in *E. coli*. But the individual contribution of PEPCK and OAA decarboxylase (ODx) is uncertain probably due to the dependency of ODx which is highly variable. For example, the genes encoding the ODx subunits are found present in *P. aeruginosa* PAO1, *P. fluorescens* Pf-5, *P. putida* KT2440 while *P. fluorescens* PfO-1, *P. putida* GB-1 and *P. putida* F1 have only the gene for alpha subunit (Stover et al., 2000; Nelson et al., 2002; Paulsen et al., 2005; Sauer and Eikmanns, 2005; Copeland et al, submitted 2005; 2007; 2008). Although high, the flux through the reverse pathway of OAA decarboxylation may not significantly affect the flux of OAA into other pathways as the PEP to OAA forward flux could still be much higher (85%).

In general, perturbation leading to *ppc* overexpression in *E. coli* reduced acetic acid secretion under aerobic conditions (Farmer and Liao, 1997) while in *C. glutamicum* improved the glutamate production under specific experimental conditions (Delaunay et al., 1999). Interestingly in catabolically diverse *P. fluorescens*, *ppc* overexpression apart from enhancing the anaplerotic pathways and improving the cellular metabolic status characteristically redistributed the glucose flux between phosphorylative and direct oxidation pathways of glucose catabolism. This phenomenon is also well-supported by the alterations observed in metabolites and the related enzyme activities. Fluxes of these branch pathways could provide further insight into the control of central metabolism.